Vinculin associates with endothelial VE-cadherin junctions to control force-dependent remodeling

Stephan Huveneers,[1] Joppe Oldenburg,[1] Emma Spanjaard,[1,2] Gerard van der Krogt,[1] Ilya Grigoriev,[3] Anna Akhmanova,[3] Holger Rehmann,[2] and Johan de Rooij[1]

[1]Hubrecht Institute for Developmental Biology and Stem Cell Research, University Medical Centre Utrecht, 3584 CT, Utrecht, Netherlands
[2]Department of Molecular Cancer Research, Centre of Biomedical Genetics and Cancer Genomics Centre, University Medical Centre Utrecht, 3584 CG, Netherlands
[3]Cell Biology, Faculty of Science, Utrecht University, 3584 CH, Utrecht, Netherlands

To remodel endothelial cell–cell adhesion, inflammatory cytokine- and angiogenic growth factor–induced signals impinge on the vascular endothelial cadherin (VE-cadherin) complex, the central component of endothelial adherens junctions. This study demonstrates that junction remodeling takes place at a molecularly and phenotypically distinct subset of VE-cadherin adhesions, defined here as focal adherens junctions (FAJs). FAJs are attached to radial F-actin bundles and marked by the mechanosensory protein Vinculin. We show that endothelial hormones vascular endothelial growth factor, tumor necrosis factor α, and most prominently thrombin induced the transformation of stable junctions into FAJs. The actin cytoskeleton generated pulling forces specifically on FAJs, and inhibition of Rho-Rock-actomyosin contractility prevented the formation of FAJs and junction remodeling. FAJs formed normally in cells expressing a Vinculin binding-deficient mutant of α-catenin, showing that Vinculin recruitment is not required for adherens junction formation. Comparing Vinculin-devoid FAJs to wild-type FAJs revealed that Vinculin protects VE-cadherin junctions from opening during their force-dependent remodeling. These findings implicate Vinculin-dependent cadherin mechanosensing in endothelial processes such as leukocyte extravasation and angiogenesis.

Introduction

Stable endothelial cell–cell junctions, mediated by vascular endothelial cadherin (VE-cadherin) in association with p120-, β-, γ-, and α-catenin, are important for maintaining vascular barrier function, whereas controlled remodeling (disruption) of endothelial junctions is crucial for processes such as leukocyte extravasation and sprouting angiogenesis (Dejana et al., 2008; Vestweber et al., 2009). Constitutively disturbed endothelial junctions are often found in pathophysiological conditions such as inflammation, vascular leakage, atherosclerosis, and tumor-associated angiogenesis (Baluk et al., 2005; Weis, 2008). Endothelial permeability factors and angiogenic growth factors, such as vascular endothelial growth factor (VEGF), TNF, and thrombin, transiently remodel junctions (Dejana et al., 2008; Vestweber et al., 2009; Fernandez-Borja et al., 2010; Carmeliet and Jain, 2011) through signaling pathways that mediate phosphorylation and endocytosis of the VE-cadherin complex (Esser et al., 1998; Angelini et al., 2006; Gavard and Gutkind, 2006).

Next to these signal transduction pathways, changes in the actin cytoskeleton play a significant role in endothelial junction remodeling: increased actomyosin contraction is involved in the onset of sprouting angiogenesis (Abraham et al., 2009; Fischer et al., 2009) and important for leukocyte transendothelial migration (Dudek and Garcia, 2001; Mammoto et al., 2008). Moreover, thrombin, VEGF, and TNF raise actomyosin contractility through activation of the small GTPase RhoA (Shasby et al., 1997; van Nieuw Amerongen et al., 2000; Zeng et al., 2002; McKenzie and Ridley, 2007; Bryan et al., 2010). Increased extracellular matrix rigidity raises cytoskeletal tension (de Rooij et al., 2005) and increases endothelial junction disruption by thrombin (Krishnan et al., 2011). Thus, increased actomyosin-based tension at endothelial cell–cell junctions is an important

J. Oldenburg and E. Spanjaard contributed equally to this paper.

Correspondence to Stephan Huveneers: s.huveneers@hubrecht.eu; and Johan de Rooij: j.derooij@hubrecht.eu

Abbreviations used in this paper: AJ, adherens junction; CCD, charge-coupled device; FA, focal adhesion; FAJ, focal adherens junction; HMEC-1, human dermal microvascular endothelial cell; HUVEC, human umbilical vein endothelial cell; IF, immunofluorescence; shRNA, short hairpin RNA; VBS, vinculin binding site; VE-cadherin, vascular endothelial cadherin; VEGF, vascular endothelial growth factor.

The Rockefeller University Press $30.00
J. Cell Biol. Vol. 196 No. 5 641–652
www.jcb.org/cgi/doi/10.1083/jcb.201108120

factor in their hormone-induced remodeling (Moy et al., 1996). In contrast, however, in the absence of hormones, VE-cadherin–based junctions stabilize and grow with increasing tension (Liu et al., 2010), and similarly, epithelial cadherin-based junctions respond to increasing force by a proportional reinforcement (le Duc et al., 2010). This indicates an intricate interplay between chemical signals and cytoskeletal forces to control remodeling of endothelial junctions.

It is evident that cadherin complexes play an important role in force transmission during actomyosin-dependent epithelial remodeling in vivo (He et al., 2010; Rauzi et al., 2010). From previous work, however, it remains unclear how F-actin is linked to the VE-cadherin complex molecularly (Weis and Nelson, 2006). α-Catenin plays a central role, but additional proteins such as Eplin and Vinculin are expected to be involved as well (Drees et al., 2005; Yamada et al., 2005; Abe and Takeichi, 2008). Recently it was found that cadherin complexes not only transmit force but can also act as active mechanosensors, and Vinculin was shown to be involved in this function (le Duc et al., 2010; Ladoux et al., 2010). Earlier, VE-cadherin was reported to take part in a mechanosensory complex that is activated when endothelial cells are placed under conditions of fluid shear stress (Tzima et al., 2005). Collectively, these observations pose the possibility that cadherin complexes not only fulfill a structural role, but that molecular events at the cadherin complex are actively involved in force-dependent junction remodeling.

Here we use various live imaging approaches and mutational analysis of the VE-cadherin complex to uncover where cytoskeletal forces apply on endothelial junctions, and how this is involved in junction remodeling induced by endothelial hormones. We identify two molecularly distinct VE-cadherin–based junctions, one involved in adhesion maintenance and one involved in junction remodeling. Vinculin precisely demarcates the remodeling junctions, which are induced by endothelial hormones dependent on increased cytoskeletal pulling force. Vinculin recruitment is not absolutely required for junction formation, maintenance, or remodeling, but Vinculin functions to protect endothelial junctions from opening during force-dependent remodeling. These data show that Vinculin-dependent mechanosensing is conserved between VE-cadherin and E-cadherin and implicate this function in processes that entail endothelial junction remodeling such as leukocyte extravasation and angiogenic sprouting.

Results

Remodeling endothelial cell–cell junctions are molecularly and phenotypically distinct junctions that attach to radial actin bundles and contain Vinculin

Live imaging of VE-cadherin–GFP (characterized in Allingham et al., 2007) in untreated confluent monolayers of primary human umbilical vein endothelial cells (HUVECs) shows that HUVECs are very motile and that their cell–cell junctions are disrupted and reform at a high frequency (Video 1). At these remodeling junctions, perpendicular VE-cadherin orientations appear at the rear of migrating cells in the monolayer, as well as between nonmigrating cells that seem to pull on their shared cell–cell junctions. To investigate the underlying dynamics of the actin cytoskeleton, we performed dual-color live imaging of Lifeact-mCherry (characterized in Riedl et al., 2008) and VE-cadherin–GFP (Fig. 1 a). Stable, mature junctions are marked by faint cortex F-actin, and are aligned by thick parallel actin bundles that do not overlap with VE-cadherin (Fig. 1 a and Video 2, left). In contrast, remodeling junctions showing perpendicular VE-cadherin orientation are attached to radial actin bundles from both cells participating in the cell–cell junction (Fig. 1 a and Video 2, right). Thus, within an unstimulated endothelial monolayer in 2D culture, two types of VE-cadherin adhesions can be distinguished: stable, mature junctions that are aligned by, but not connected to, parallel actin bundles; and active, remodeling junctions that are connected to radial actin bundles and show a perpendicular orientation of VE-cadherin.

To investigate the molecular differences between stable and remodeling junctions, we used immunofluorescence (IF) to stain for proteins previously implicated in the attachment of cell–cell junctions to the actin cytoskeleton. The most striking observation in HUVECs is the exclusive presence of Vinculin in perpendicular oriented, VE-cadherin–marked cell–cell junctions that are contacted by radial F-actin bundles (Fig. 1 b). In junctions aligned by parallel actin bundles, which are most likely stable junctions, there is a striking absence of Vinculin. Because Vinculin is also a prominent member of focal adhesions (FAs), the sites of integrin-mediated adhesion to the extracellular matrix (Humphries et al., 2007), and because integrin adhesions have been found associated with cell–cell junctions in several instances (Chattopadhyay et al., 2003; Yamada and Nelson, 2007), we next investigated whether other FA members besides Vinculin are present in perpendicular oriented cell–cell junctions in HUVECs. However, even when FAs are located close to endothelial junctions, we find no colocalization of the FA proteins phospho-Paxillin (pY118), phospho-FAK (pY397), or Talin with VE-cadherin at perpendicularly oriented junctions (Fig. 1 c and Fig. S1, a–c). Co-IF stainings of Paxillin and Vinculin in HUVECs (Fig. S1 d) and human dermal microvascular endothelial cells (HMEC-1s; Fig. S1, e and f) show that Vinculin is located at integrin- as well as cadherin-based adhesions, which are clearly separate structures. Vinculin localization at perpendicular cell–cell junctions was confirmed using an alternative Vinculin-specific antibody (Fig. S1 g). Collectively, these results show that Vinculin marks a molecularly (presence of Vinculin) and morphologically (perpendicular orientation) distinct subset of VE-cadherin adhesions, which are attached to radial actin bundles and display increased remodeling compared with stable adherens junctions that are paralleled by actin bundles and do not contain Vinculin. Similar looking adherens junctions were previously recognized in epithelial cells and fibroblasts by Yonemura et al. (1995), who termed them spot-like adherens junctions; by Vasioukhin et al. (2000) during epithelial junction formation, who named them zipper-like junctions; by Millán et al. (2010) in endothelial cells,

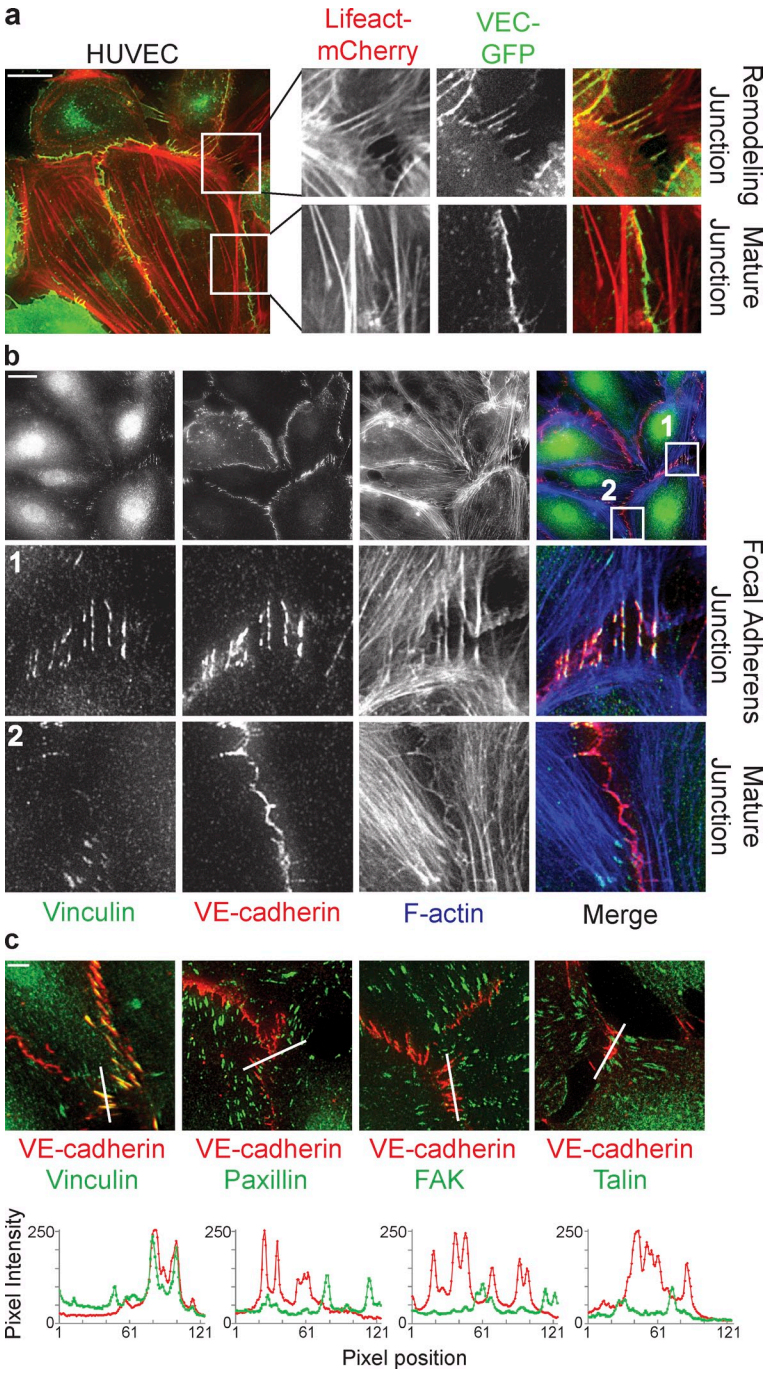

Figure 1. **Vinculin marks distinct, remodeling cell–cell junctions attached to radial actin bundles.** (a) Still images and enlarged views from time-lapse recordings (Video 2) showing perpendicularly oriented remodeling cell–cell junctions and linear stable/mature cell–cell junctions in a monolayer of HUVECs expressing VE-cadherin–GFP (green) and the F-actin probe Lifeact-mCherry (red). (b) IF images of HUVECs stained for Vinculin (green), VE-cadherin (red), and F-actin (blue) showing specific colocalization of Vinculin with perpendicular remodeling junctions, the FAJs (middle), and the absence of Vinculin from stable/mature linear junctions (bottom). (c, top) Merged IF images of HUVECs stained for Vinculin, phospho-Y118-Paxillin, phospho-Y397-FAK, or Talin (green) together with VE-cadherin (red). (c, bottom) Accompanying fluorescence intensities along the depicted lines showing that Vinculin, but not Paxillin, FAK, or Talin (green lines) colocalize with VE-cadherin (red lines) at FAJs. See also Fig. S1 for details. Bars: (a and b) 20 µm; (c) 5 µm.

who named them discontinuous adherens junctions; and very recently by Taguchi et al. (2011) in epithelial cells, who called them punctate adherens junctions. It is very well possible that all of these described morphologically distinct junctions are apparitions of the same adhesive structure. Here we show that the morphologically distinct junctions we studied also differ from stable adherens junctions (AJs) in their stability, molecular complexity, and biophysical properties (see the following paragraphs). Therefore, we propose to collectively call these perpendicularly oriented Vinculin-containing junctions focal adherens junctions (FAJs) to emphasize their distinction from stable AJs and to emphasize their analogy to FAs, the sites where integrins connect to actin bundles.

Endothelial hormones induce the formation of FAJs

Remodeling of endothelial junctions is tightly regulated by endothelial permeability factors during processes like leukocyte extravasation and angiogenesis. To investigate if these factors affect FAJ formation in HUVECs, we analyzed the organization of VE-cadherin, Vinculin, and F-actin. As shown by IF in Fig. 2 a (white arrows), the pro-angiogenic hormone VEGF moderately increases the number of FAJs at the termini of short actin bundles, which are most prominent after 4 h. Furthermore, TNF induces elongation and alignment of endothelial cells, which is clearest after 24 h. Vinculin-containing FAJs appear at the tips of long actin bundles in the "front" and "rear" of these cells.

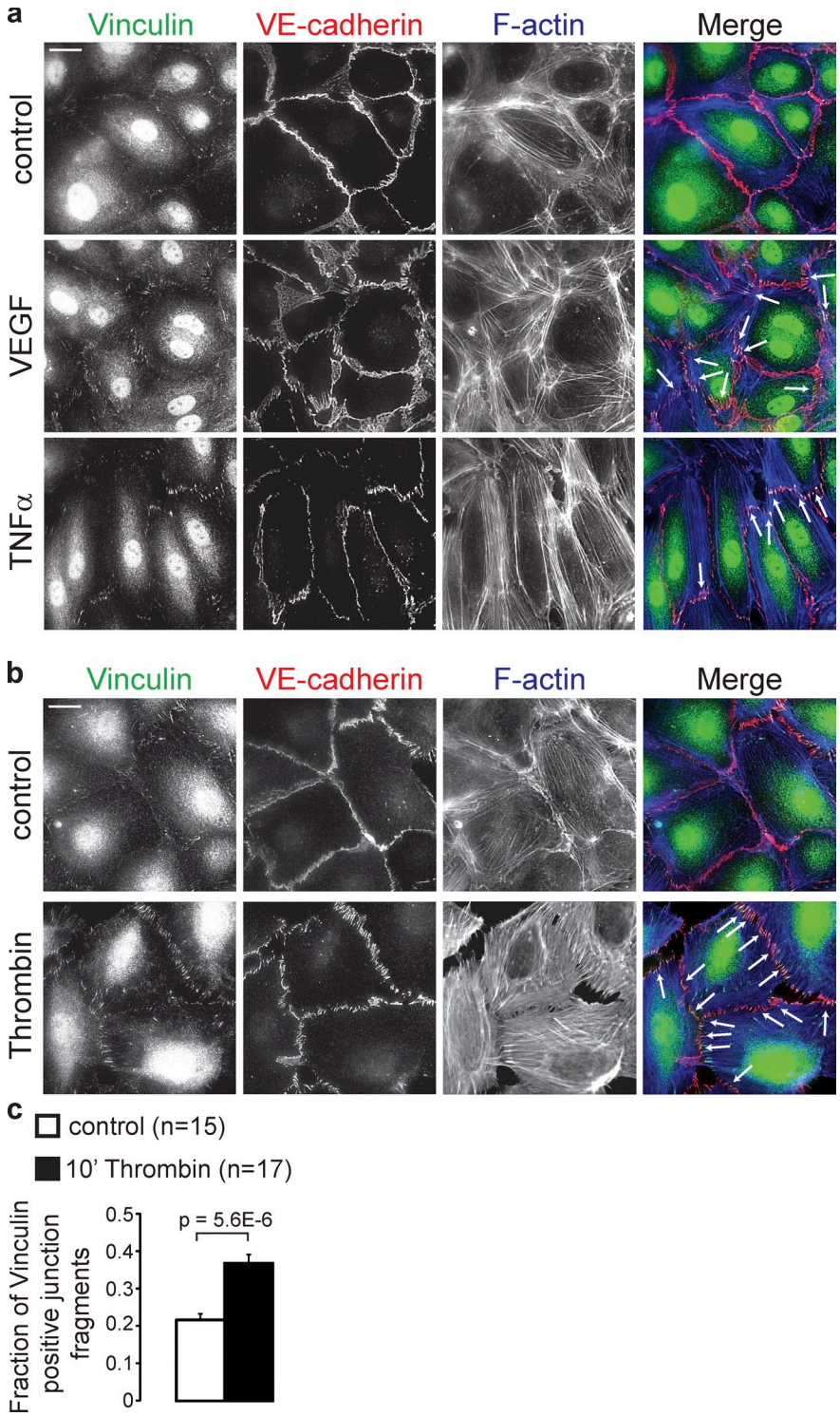

Figure 2. **VEGF, TNF, and Thrombin induce the formation of FAJs.** (a) IF images of Vinculin (green), VE-cadherin (red), and F-actin (blue) in HUVEC monolayers that were left untreated (control) or stimulated with VEGF for 4 h or TNF for 24 h. Arrows point to FAJs that are characteristic for VEGF and TNF treatments. Bar, 20 µm. (b) IF images of HUVECs that were untreated or stimulated with thrombin for 10 min, and stained as in a. Please note the strong induction of FAJs (arrows) by thrombin. Bar, 20 µm. (c) Graph shows a quantification of the fraction of Vinculin-positive junction fragments (detected by automated image segmentation based on VE-cadherin signal, see Materials and methods) in control (n = 15 images) and in thrombin (n = 17 images)-treated HUVECs of two independent experiments. Values are averages ± SEM (error bars). P-value was calculated with a two-tailed, homoscedastic Student's t test.

The most prominent and rapid effect is induced by the permeability factor thrombin: within 10 min, VE-cadherin–GFP in initially stable junctions massively reorients into perpendicular, remodeling adhesions (Video 3). Triple IF reveals a strongly increased number of Vinculin-positive actin-anchored FAJs (Fig. 2 b). Automated image quantification (see Materials and methods) demonstrates that thrombin increases the percentage of Vinculin-containing junction fragments by approximately twofold (Fig. 2 c). Live imaging of p120-catenin–mCherry and Vinculin-GFP in HUVEC and HMEC-1 cells shows the rapid recruitment of Vinculin to junctions after thrombin. Specifically, those junctions that are being disrupted are the ones that accumulate Vinculin (Fig. 3 a, Fig. S2, and Video 4).

The formation of FAJs may involve a transformation of existing stable junctions or the recruitment of a new pool of cadherin complexes. To distinguish between these possible mechanisms, we followed α-catenin–Dendra2, photoswitched in stable junctions, during thrombin-induced FAJ

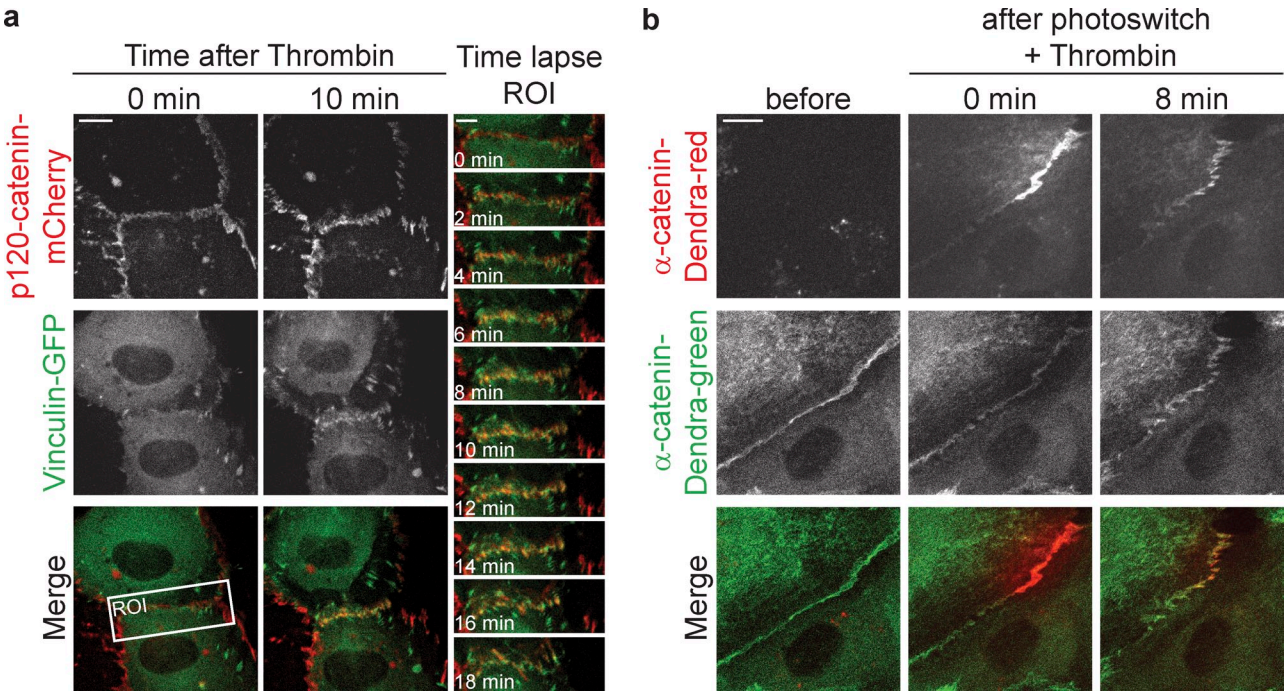

Figure 3. **Thrombin induces FAJs formation by transformation of stable AJs.** (a) Time-lapse images of HUVECs expressing p120-catenin–mCherry (red) and Vinculin-GFP (green) after thrombin stimulation. Merged images on the right highlight the rapid recruitment of Vinculin during thrombin-induced junction remodeling at the region of interest. See corresponding Video 4 for the ∼1-h time-lapse recording. (b) Time-lapse images of HUVECs expressing α-catenin–Dendra2 before and after photoswitching a fraction of a stable junction using a 405-nm confocal laser followed by thrombin-induced FAJ formation. See corresponding Video 5 for an 8-min time-lapse recording. Bars: (a, left) 10 µm; (a, right) 5 µm; (b) 10 µm

formation. These experiments show that a significant portion of the switched α-catenin molecules is maintained at the junctions during their transition from stable AJs to remodeling FAJs (Fig. 3 b and Video 5). Thus, we conclude that FAJs are formed by a transformation of existing AJs, which involves molecular and physical changes, including Vinculin recruitment and radial actin attachment, of cadherin complexes that remain present throughout the transition process.

Actomyosin contraction generates pulling forces specifically on FAJs and is required for their formation and junction remodeling

Inhibition of Rho signaling leads to a strong inhibition of VEGF, TNF, and thrombin-induced junction remodeling (van Nieuw Amerongen et al., 2000; McKenzie and Ridley, 2007; Bryan et al., 2010). To investigate whether actomyosin contractility is required for the formation of FAJs, the remodeling subset of endothelial junctions, we blocked the Rho–Rock–actomyosin pathway in HUVECs at the level of Rho (using 1 µg/ml C3 transferase for 4 h), Rock (using 10 µM Y-27632 for 10 min), or myosin-II (using 100 µM blebbistatin for 30 min). Inhibiting this pathway causes a complete loss of FAJs in HUVECs, as judged by the loss of junctional Vinculin, the disappearance of junction-connected radial actin bundles, and the increase in F-actin at the cell cortex (Fig. 4, a and b; and Fig. S3). Inhibition of this pathway also induces a significant loss of thrombin-induced junction remodeling as judged by live cell imaging of Vinculin-GFP and p120-catenin–mCherry–expressing HUVECs (Video 6). Importantly, treating HUVECs with a VE-cadherin function-blocking antibody (clone 75 used at 12.5 µg/ml for 2 h) also results in a complete loss of FAJs (Fig. 4 a). These experiments demonstrate that actomyosin-generated cytoskeletal tension, anchored at VE-cadherin–dependent cell–cell junctions, underlies the formation of FAJs, and subsequent remodeling of endothelial cell–cell adhesion.

To reveal cell–cell junctions susceptible to tension from attached actin bundles, we used low doses of the barbed end actin capping agent Cytochalasin D, a method previously validated by the Nelson laboratory (Yamada and Nelson, 2007). As shown in Fig. 5 a, Cytochalasin D induces a rapid (within 30–60 s) displacement of cell–cell junction markers in Vinculin-GFP– and p120-catenin–mCherry–expressing HUVECs. The p120-catenin–mCherry signal from FAJs translocates radially into the cell to a mean distance of 11.18 µm from the original junction after 60 s of Cytochalasin D treatment (Fig. 5, a and b; and Video 7, left). In contrast, Vinculin-negative junction markers hardly show any displacement after Cytochalasin D (0.88 µm in 60 s; Fig. 5, a and b; and Video 7, right). The same results were obtained in HMEC-1 cells (Fig. S4). These results show that Vinculin-containing FAJs are biophysically distinct from Vinculin-negative AJs. The nature of the displacement of the FAJs in the direction of the attached contractile F-actin bundles suggests that they experienced pulling forces that could not be sustained by the cell–cell junction complex in the presence of Cytochalasin D.

To investigate whether the actin-attached FAJs indeed experience mechanical tension under normal growth conditions, we performed laser ablation in HUVECs expressing

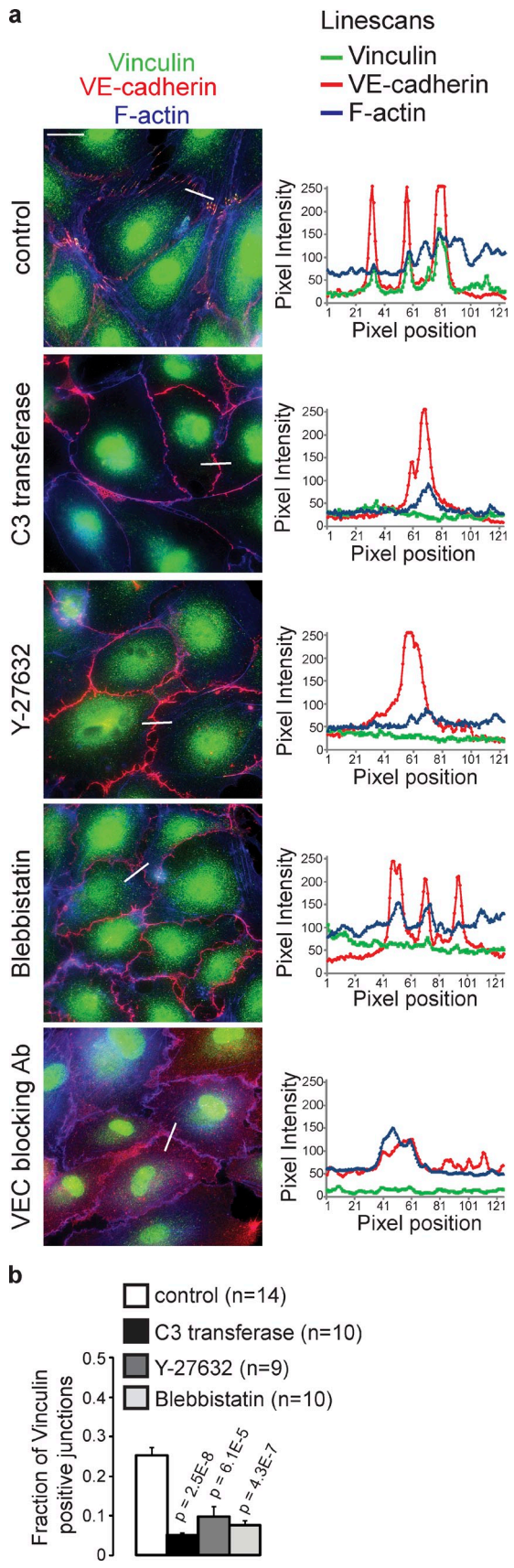

Figure 4. **FAJs require actomyosin contraction for their formation.** (a) IF images of HUVECs stained for Vinculin (green), VE-cadherin (red), and F-actin (blue) that were treated with membrane-permeable C3 transferase for 4 h to inhibit Rho, Y-27632 for 10 min to inhibit Rock, blebbistatin for 30 min to inhibit myosin activities, or VE-cadherin blocking antibody for 2 h. Line scans on the right show intensities of Vinculin, VE-cadherin, and F-actin signal across indicated junctions. See also Fig. S3 for details. Bar, 20 µm. (b) Quantification (as in Fig. 2 c) of the fraction of Vinculin-positive junction fragments in HUVECs treated with C3 transferase (n = 10 images), Y-27632 (n = 9 images), or blebbistatin (n = 10 images) compared with control (n = 14 images) of two independent experiments. Values are averages ± SEM (error bars). P-values were calculated with a two-tailed, homoscedastic Student's t test.

VE-cadherin–GFP and Lifeact-mCherry at regions where radial actin bundles were associated with FAJs. Immediately after the radial actin bundles connected to the FAJs are severed by laser ablation, the junctions translocate in the direction of pulling by the interacting nonablated cell (Fig. 5 c and Video 8). This experiment was performed multiple times and a representative time lapse is shown. The directionality and extent of junction translocation depends on the complexity of the actin network of both cells, impeding a meaningful quantification. These data clearly show that the radial actin bundle–connected, Vinculin-containing FAJs experience tension generated by actomyosin-based pulling forces.

It was recently shown that the apical adherens junctions in epithelial cells also increase junctional Vinculin levels in an actomyosin-dependent manner (Yonemura et al., 2010). This was attributed to a stretch-induced conformational change in α-catenin exposing a shielded binding site for Vinculin. This could be monitored by the α18 antibody that specifically recognizes an epitope adjacent to the Vinculin binding site (Yonemura et al., 2010). In control and thrombin-stimulated HUVECs, however, IF staining with the same α18 antibody shows a pattern that is very similar to VE-cadherin (Fig. 5 d), and is not confined to FAJs like Vinculin (Fig. 5 e). Although further comparison, beyond the scope of this paper, is warranted, this result indicates that the molecular details of the FAJ in endothelial cells are not the same as those of the apical junction in epithelial cells.

Junctional Vinculin is not required for linking VE-cadherin to F-actin, but restrains force-dependent junction disruption by thrombin

F-actin organization and myosin-based contraction strongly depend on the coupling of actomyosin to integrin-based FAs (Puklin-Faucher and Sheetz, 2009), and Vinculin depletion affects both integrin adhesion (Rodríguez Fernandez et al., 1993) and actomyosin contractility (Mierke et al., 2008). Consequently, depletion of total cellular Vinculin cannot be used to investigate its function in the actomyosin-dependent regulation of cell–cell adhesion. To specifically interfere with Vinculin's recruitment to cell–cell junctions, and leave its function at FAs intact, we substituted the vinculin binding site (VBS) of α-catenin (aa 302–402, based on Yonemura et al., 2010; Watabe-Uchida et al., 1998) with the homologous part from Vinculin (note: Vinculin is the closest homologue of α-catenin; Fig. 6 a). To control this hybrid α-catenin, we first tested its functionality in DLD1-R2/7 α-catenin–negative cells. Just like wild-type α-catenin-GFP, α-catenin–ΔVBS–GFP expression restores cell–cell adhesion in

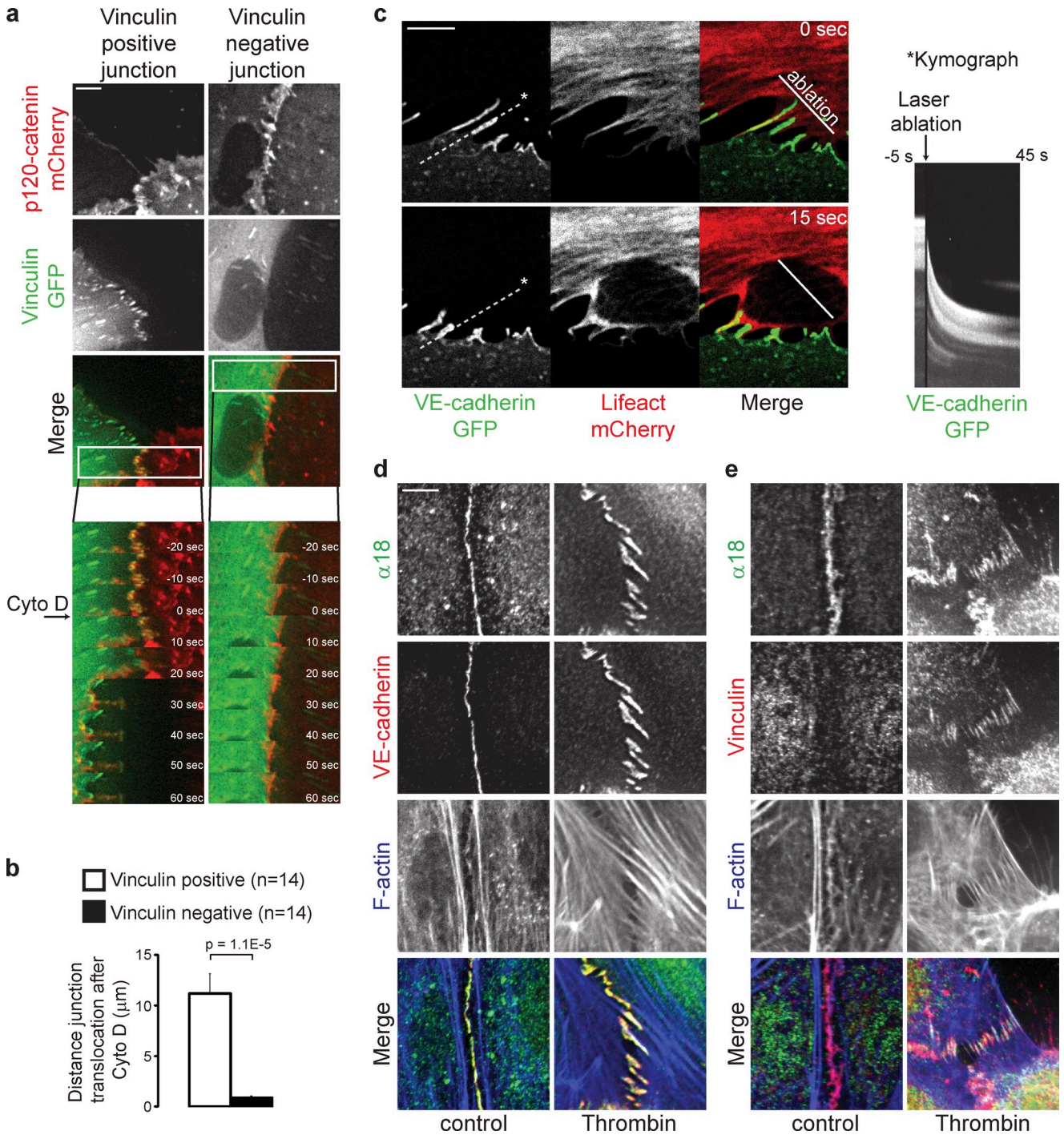

Figure 5. **FAJs are tensile junctions.** (a) Time-lapse images of HUVECs expressing p120-catenin–mCherry (red) and Vinculin-GFP (green) during treatment with a low dose of Cytochalasin D. Note the specific and rapid displacement of the Vinculin-containing junction, whereas the Vinculin-negative junction does not move in this time period. See corresponding Video 7 for 16-min time-lapse recordings. (b) Quantification of the mean distance of translocation ± SEM of the p120-catenin signal within 60 s after Cytochalasin D treatment of Vinculin-positive junctions (n = 14) and Vinculin-negative junctions (n = 14) from five different experiments as determined by manual measurements in ImageJ. P-value was calculated with a two-tailed, homoscedastic Student's t test. (c) Time-lapse images of FAJs in HUVECs expressing VE-cadherin–GFP (green) and Lifeact-mCherry (red), before and 15 s after laser ablation at the indicated region. See corresponding Video 8 for an ∼1-min time-lapse recording, which is representative of multiple experiments. The image on the right is a kymograph showing the intensity of VE-cadherin–GFP in time along the dotted line (shown is the maximum intensity pixel of a 10-pixel-wide line). (d and e) IF images of control and thrombin-treated HUVECs stained with the conformation-sensitive α18 rat monoclonal antibody for α-catenin (green), phalloidin for F-actin (blue), and antibodies for VE-cadherin (d) or Vinculin (e; red). Bars: (a) 5 µm; (c) 5 µm; (d and e) 20 µm.

DLD1-R2/7, and we observed no obvious differences in their AJ organization, even though these junctions are completely devoid of Vinculin (Fig. S5 a). This indicates that α-catenin–ΔVBS is fully functional in its capacity to provide structural support for E-cadherin–based cell–cell adhesion even though it is unable to recruit Vinculin to cell–cell junctions.

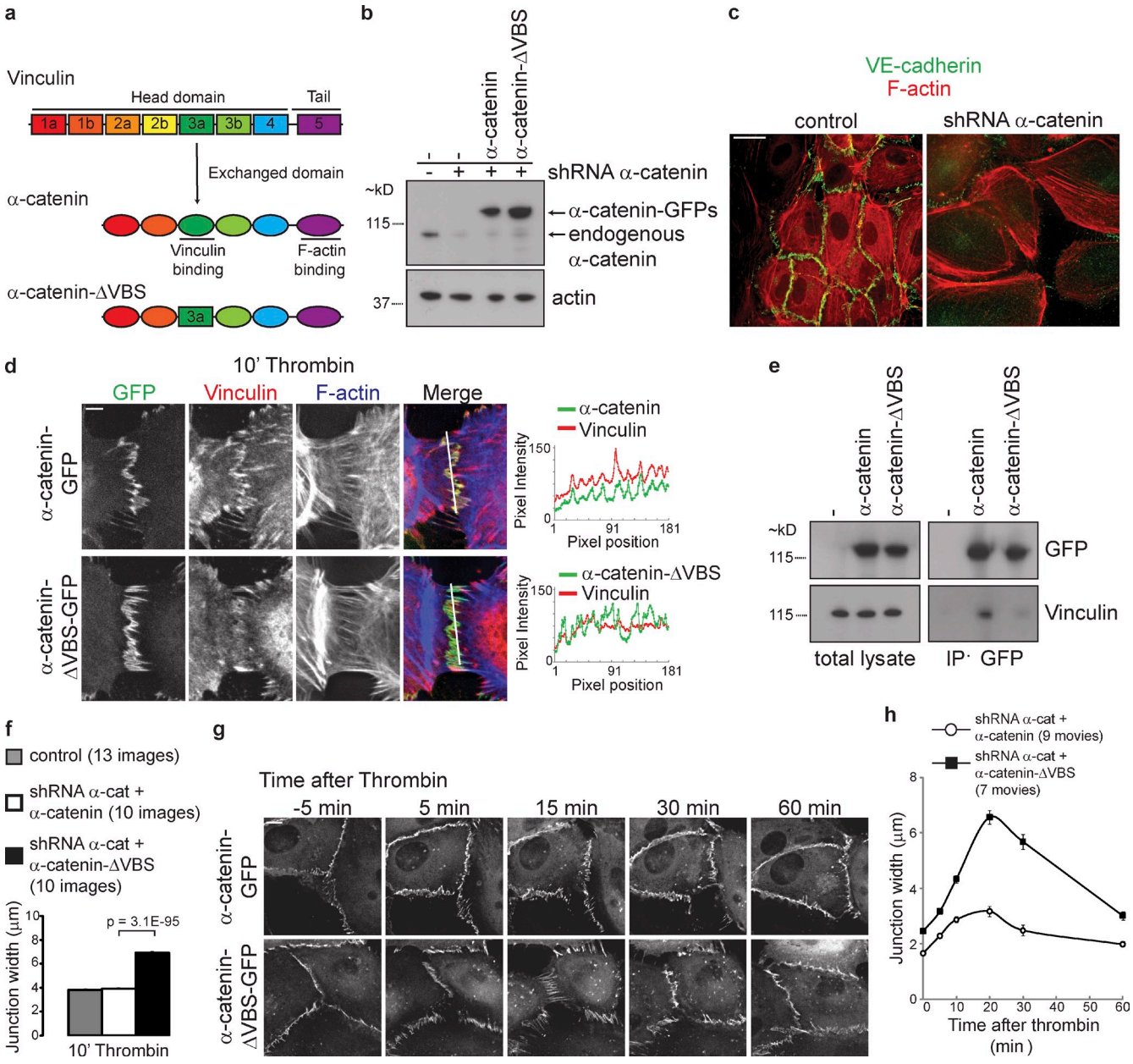

Figure 6. **Junctional Vinculin restrains force-dependent junction disruption by thrombin.** (a) Schematic representation of Vinculin and α-catenin to illustrate which homolog's domain (dark green) was swapped to generate a hybrid α-catenin–ΔVBS that is unable to associate with Vinculin. (b) Representative Western blot analysis of α-catenin and actin in lysates of HUVECs transduced with α-catenin shRNAs and rescued by α-catenin–GFP or α-catenin–ΔVBS–GFP. (c) IF images of control HUVECs and HUVECs transduced with lentiviral shRNA against human α-catenin stained for VE-cadherin (green) and F-actin (red). Bar, 20 µm. (d) IF images of α-catenin shRNA-transduced HUVECs rescued with wild-type α-catenin–GFP (top) or α-catenin–ΔVBS–GFP (bottom) that were stimulated with thrombin for 10 min, and stained for Vinculin (red) and F-actin (blue). Colocalization of Vinculin with α-catenin–GFP or α-catenin–ΔVBS–GFP was analyzed by line scans displaying signal intensity across the FAJs as indicated. Bar, 10 µm. (e) Representative Western blot analysis of GFP and Vinculin in total lysates and in GFP immunoprecipitations from thrombin-stimulated HUVECs expressing indicated GFP constructs. (f) Quantification of the average junction width ± SEM after 10 min of thrombin treatment as measured using ImageJ in IF stainings of two independent experiments of control HUVECs (13 images, *n* = 382 junction width measurements), α-catenin shRNA–transduced HUVECs rescued with α-catenin–GFP (10 images, *n* = 987), or α-catenin–ΔVBS–GFP (10 images, *n* = 1,201). P-value was calculated with a two-tailed, homoscedastic Student's *t* test. (g) Time-lapse images of α-catenin shRNA transduced HUVECs rescued with α-catenin–GFP (top) or α-catenin–ΔVBS–GFP (bottom) that were stimulated with thrombin, showing that thrombin induces wider remodeling junctions that persist longer in α-catenin–ΔVBS–GFP cells than in α-catenin–GFP cells. See corresponding Video 10 for ∼3-h time-lapse recordings. Bar, 10 µm. (h) Quantification of the mean junction width ± SEM after thrombin of α-catenin–GFP (nine time-lapse recordings) and α-catenin–ΔVBS–GFP (seven time-lapse recordings) junctions of two independent experiments as measured in time-lapse recordings using ImageJ. The number of junction width measurements (*n* value) of α-catenin–GFP and α-catenin–ΔVBS–GFP at time points 0, 10, 15, 20, 30, and 60 min after thrombin were 208, 409; 212, 375; 143, 311; 67, 180; 69, 126; and 149, 230, respectively.

To study the role of junctional Vinculin in HUVECs, we silenced human α-catenin by lentiviral short hairpin RNAs (shRNAs; Fig. 6 b) to levels that abolish cell–cell adhesion (Fig. 6 c) and rescued junctions by expression of mouse α-catenin–GFP or α-catenin–ΔVBS–GFP (Fig. 6 b). Both α-catenin variants restore cell–cell adhesion to a very similar

extent, as shown by their junctional localization and dynamics (Video 9). Surprisingly, in both α-catenin and α-catenin–ΔVBS–rescued HUVECs, FAJs are also formed at similar frequencies. Importantly, however, Vinculin was not detectable in FAJs in α-catenin–ΔVBS–GFP–rescued cells (Fig. 6 d). In this context, we also investigated the interaction of α-catenin–GFP and α-catenin–ΔVBS–GFP with endogenous Vinculin in thrombin-stimulated HUVECs biochemically. Vinculin coimmunoprecipitated with α-catenin–GFP, and indeed its interaction with α-catenin–ΔVBS–GFP was strongly perturbed (Fig. 6 e). The detection of the interaction of α-catenin and Vinculin is not very abundant, just like we observe for the interaction of Vinculin with the E-cadherin complex in MDCK cells (le Duc et al., 2010). Together, these data confirm the structural functionality of the α-catenin–ΔVBS mutant while showing that it lacks the capacity to recruit Vinculin to junctions. Also, they demonstrate that Vinculin is not required for the coupling of radial actin bundles to cell–cell junctions, the formation of FAJs, and induction of junction remodeling. However, after thrombin, Vinculin-devoid FAJs are clearly enlarged compared with Vinculin-containing FAJs (Fig. 6 d). Quantification shows a strong increase in the width of cell–cell junctions after thrombin in α-catenin–ΔVBS–GFP–rescued cells (6.9 µm) compared with α-catenin–GFP–rescued (3.9 µm) and wild-type cells (3.8 µm; Fig. 6 f). In α-catenin–ΔVBS–GFP–rescued cells, thrombin induces junction disruption more severely, and junctions fail to return to their stable state for a prolonged time (Fig. 6 g and Video 10). Consequently, the increased width of remodeling junctions in α-catenin–ΔVBS–GFP–rescued cells persists longer in time (30 min after thrombin treatment junction width of α-catenin–ΔVBS–GFP–rescued cells was 5.7 µm vs. 2.5 µm for α-catenin–GFP; Fig. 6 h). In conclusion, these results demonstrate that VE-cadherin–dependent junctional recruitment of Vinculin is not required for the linkage of cell–cell junctions to F-actin or junction formation. This is in contrast to recent studies that used total Vinculin knockdowns (Peng et al., 2010; Taguchi et al., 2011), which likely also affected other functions of Vinculin. Instead, our data reveal a role for Vinculin in the protection against force-dependent remodeling of endothelial junctions.

Discussion

In this study, we have shown that there are two distinct types of cadherin-based junctions in endothelial cells: stable, nonremodeling AJs, and FAJs that are actively remodeling. FAJs are perpendicularly oriented with respect to the cell–cell contact plane and highlighted by the presence of Vinculin, which exactly demarcates attachment sites to radial actin bundles, and which makes these junctions molecularly distinct from stable AJs. Dependent on an increase in actomyosin generated pulling forces, endothelial permeability factors initiate the formation of FAJs from stable AJs to induce cell–cell adhesion remodeling. Vinculin recruitment by α-catenin is not needed for the formation of FAJs, or their coupling to radial F-actin bundles, but restrains force-dependent endothelial junction remodeling at these specific sites.

Vinculin recruitment to adherens junctions

Vinculin was recently identified as a myosin-dependent member of epithelial cell–cell junctions. Yonemura et al. (2010) and others (Miyake et al., 2006) showed that Vinculin is present in apical AJs, whereas our laboratory showed junctional Vinculin in the basolateral AJs of hepatocyte growth factor–stimulated MDCK cells (le Duc et al., 2010). The presence of Vinculin in a force-dependent subset of VE-cadherin–mediated endothelial junctions extends the mechanical function of Vinculin to a second member of the classical cadherin family, but there are also notable differences: apical AJs do not exist in HUVECs cultured in 2D. The presence of Vinculin in apical AJs, but not the apical junction itself, is actomyosin-dependent in epithelial cells (Yonemura et al., 2010). FAJs themselves are actomyosin-dependent structures, but do not display an increased staining with α18, the conformation-specific α-catenin antibody that specifically stains apical AJs in an actomyosin-dependent manner. Therefore, it is unlikely that Vinculin's presence at these different cell–cell junctions represents the exact same molecular mechanism. The molecular details of the mechanism that triggers Vinculin recruitment to basolateral tension building junctions is still unknown. Nevertheless, experiments with our α-catenin–ΔVBS mutant do indicate that in both epithelial apical junctions and endothelial FAJs, α-catenin is the main recruiter of Vinculin, and not β-catenin, as was found in MCF10A cells (Peng et al., 2010). Our photo-switching experiments show that α-catenin itself is most likely not displaced during Vinculin recruitment, which indicates that allosteric activation of its Vinculin binding site is involved. Clearly further study is needed to establish the exact molecular mechanism of Vinculin-recruitment to the diverse cell–cell junctions.

The function of junctional Vinculin

Downstream of its recruitment to the different cell–cell junctions, force-dependent reinforcement is one function of Vinculin that is clearly emerging. The Yap laboratory has shown that Vinculin is involved in tightening of epithelial apical junctions during their maturation (Maddugoda et al., 2007), which had also been postulated by the Takeichi and Nagafuchi laboratories (Watabe-Uchida et al., 1998; Imamura et al., 1999). In the remodeling FAJs that we have identified here, the main function of Vinculin is to protect junctions against overinduced opening by thrombin. How Vinculin accomplishes a mechanoresponse is unclear, but it could involve recruitment of actin regulators such as ARP2/3 (DeMali et al., 2002) or actin modulation activity of Vinculin itself (Wen et al., 2009; Le Clainche et al., 2010). Our current data with the α-catenin–ΔVBS mutant, which reduces Vinculin recruitment to undetectable levels, show for the first time that recruitment of Vinculin by α-catenin is not required for the link between cell–cell junctions and F-actin, not even when junctions are strongly pulled by actin bundles after thrombin. This conclusion is in sharp contrast with conclusions reached by reducing the expression of total cellular Vinculin, which resulted in a strong impairment of E-cadherin–mediated adhesion (Peng et al., 2010; Taguchi et al., 2011). Importantly, total Vinculin

depletion not only impairs cell–cell adhesion, but also affects cell–matrix adhesions and global mechanical properties of the actomyosin cytoskeleton (Rodríguez Fernandez et al., 1993; Mierke et al., 2008). Whether these different observations are caused by separate functions of Vinculin being disrupted or are interconnected needs to be established. Our data argue that total depletion of Vinculin from cells does not lead to an accurate assessment of its function in seemingly separate cellular processes. We conclude that Vinculin's function at endothelial cell–cell junctions is not needed for their formation or maintenance, but that it is specifically needed during active phases of junction remodeling by cytoskeletal force to protect junctions from opening.

Concluding remarks

In conclusion, the presence of actin-contacted FAJs and concomitant Vinculin-controlled junction remodeling through cytoskeletal pulling forces that we have identified here have strong implications for understanding angiogenic and inflammatory remodeling of the vascular endothelium, and this is likely to function similarly during junction remodeling in other tissues that express classical cadherins. If the specific protective function of Vinculin could be harnessed pharmacologically, for instance by enhancing its interaction with α-catenin, it may provide an additional strategy to treat pathologies that are caused by or entail vascular permeability.

Materials and methods

Cell culture and cells

Pooled HUVECs (cultured up to passage 6) from different donors (Lonza) and HMEC-1 were cultured in EBM-2 culture medium supplemented with EGM-2 bulletkit (Lonza) on gelatin-coated tissue flasks. DLD1-R2/7 (a gift from F. van Roy, University of Gent, Gent, Belgium; van Hengel et al., 1997) and HEK293T cells were cultured in Dulbecco's modified Eagle's medium supplemented with 10% fetal bovine serum and antibiotics.

Antibodies and other reagents

Mouse monoclonal Vinculin antibody hVIN-1 was used in Figs. 6 d, S1, and S5 a; and rabbit polyclonal Vinculin antibody was used in all other IF experiments; both were obtained from Sigma-Aldrich. Mouse monoclonal Talin 8D4 and rabbit polyclonal α-catenin antibodies were obtained from Sigma-Aldrich. Rabbit polyclonal antibodies for FAK (pY397) and paxillin (pY118) were from Invitrogen, and antibodies for VE-cadherin were from Cell Signaling Technology. Mouse monoclonal paxillin antibody clone 349 and VE-cadherin antibody clone 75 (used at 12.5 µg/ml to block VE-cadherin adhesion in Fig. 4 a) were purchased from BD, and mouse monoclonal actin antibody clone C4 was obtained from Millipore. Rabbit polyclonal clonal anti-GFP antibody was obtained from Covance. The rat α18 antibody was a gift of A. Nagafuchi (Kumamoto University, Kumamoto, Japan). Secondary antibodies coupled to Alexa Fluor 488 and Alexa Fluor 594 were obtained from Invitrogen. Promofluor 415–coupled phalloidin was from PromoKine. Blebbistatin (used at 100 µM) and Y-27632 (used at 10 µM) were from EMD, cell-permeable C3 transferase (used at 1 µg/ml in serum-free medium) from Cytoskeleton, and Cytochalasin D (used at 0.2 µg/ml) was from Sigma-Aldrich. Human plasma-derived thrombin (used at 0.2 U/ml) and Fibronectin were purchased from Sigma-Aldrich. Human recombinant $VEGF_{165}$ (used at 50 ng/ml in serum-free medium) and TNF (used at 10 ng/ml in serum-free medium) were from PeproTech.

DNA constructs and viral transductions

Adenoviral transductions of HUVECs for the experiments in Videos 1 and 3 with human VE-cadherin fused to GFP (characterized in Allingham et al., 2007; the virus was a gift from J. van Buul, Sanquin, Amsterdam, Netherlands) were performed using a Virapower Adenoviral Expression system (Invitrogen). For lentiviral transductions (all other experiments), human VE-cadherin–GFP was cut out of a peGFP–VE-cadherin vector (provided by J. van Buul) using NdeI and XbaI restriction enzymes and cloned into a self-inactivating lentiviral pLV-CMV-ires-puro vector using the NdeI and NheI restriction sites. The same cloning strategy was used to transfer full-length mouse p120-catenin–mCherry from a pmCherry-n1 vector (le Duc et al., 2010) and full-length mouse α-catenin–GFP from a peGFP-c1 vector. The GFP tag of α-catenin was replaced by Dendra2 derived from a pDendra2-c1 vector (Evrogen) using NdeI and SalI restriction enzymes to generate pLV–CMV–α-catenin–Dendra2. To generate α-catenin–ΔVBS–GFP, the structure of α-catenin was modeled on top of the crystal structure of Vinculin (as published by Bakolitsa et al., 2004) to precisely define α-helices and determine their boundaries to choose the correct sites to perform the domain swap. An EagI site was introduced at the start of the swapped sequence (aa 302 of α-catenin), and the homologous domain from chicken Vinculin was amplified by PCR and cloned into this EagI site and the unique ScaI site at the end of the Vinculin-binding domain (aa 402 of α-catenin). The resulting amino acid sequence is SEERFRPVGQ at the N-terminal boundary and TTTPILVLIEAAK at the C-terminal boundary of the swapped domain. Lentiviral expression constructs pRRL-Lifeact-mCherry and pRRL-Vinculin-GFP were a gift of O. Pertz (University of Basel, Basel, Switzerland). shRNA encoding lentiviral vectors targeting human α-catenin were MISSION TRC1 clones (TRC nos. 0000062653, 0000062654, and 0000062657) from Sigma-Aldrich. Lentiviral particles were isolated from the supernatant of HEK293 cells transiently transfected with third-generation packaging constructs and the lentiviral expression vectors. HUVECs were infected with supernatant containing lentiviral particles in the presence of 8 µg/ml polybrene overnight. To generate the rescue cell types in Fig. 6, HUVECs were first transduced with a pool of lentiviral shRNAs for human α-catenin, and at least 24 h later transduced with α-catenin–GFP or α-catenin–ΔVBS–GFP–containing lentivirus as indicated.

Wide-field IF and live cell microscopy

For live-cell microscopy, cells were plated on Lab-Tek chambered 1.0 borosilicate coverglass slides coated with 3 µg/ml Fibronectin and cultured in EBM-2 culture medium supplemented with EGM-2 bulletkit. For IF stainings, cells were plated on coverslips coated with 3 µg/ml Fibronectin, and after culture fixed for 15 min in 4% paraformaldehyde, permeabilized with 0.4% Triton X-100 for 5 min, and blocked in 2% BSA for 1 h. Phalloidin, primary, and secondary antibody stainings were performed in 2% BSA for 1 h, and coverslips were mounted in Mowiol4-88/DABCO solution (Sigma-Aldrich). Live (at 37°C) and fixed cells were imaged using an inverted research wide-field microscope (Eclipse Ti; Nikon) with perfect focus system, equipped with a 20× 0.75 NA Plan-Apochromat VC differential interference contrast (dry; for the experiments in Videos 1 and 9) or a 60× 1.49 NA Apochromat total internal reflection fluorescence (oil) objective lens (all other wide-field experiments), a microscope cage incubator (OkoLab), and an EM charge-coupled device (CCD) camera (Andor Technology) controlled with NIS-Elements Ar 3.2 software. For the Dendra2 photoswitching experiments in Fig. 3 b and Video 5, a C1 confocal box (Nikon) and 405-nm, 488-nm, and 594-nm lasers were used that are connected to the wide-field Nikon microscope system. All images were enhanced for display with an unsharp mask filter or background subtraction by rolling ball, and brightness/contrast adjustments in ImageJ (National Institutes of Health). Line scans were made from original images using MetaMorph 7.5 software.

Laser ablation and spinning disc live cell microscopy

For laser ablation experiments in Fig. 5 c and Video 8, cells were plated on glass coverslips coated with 3 µg/ml Fibronectin and cultured in EBM-2 culture medium supplemented with EGM-2 bulletkit. Laser ablation was performed on an inverted research microscope (Eclipse Ti-E; Nikon) with a perfect focus system, equipped with a CFI S Fluor 100× 1.3 NA oil objective lens (Nikon), a spinning disc confocal microscope (CSU-X1-A1; Yokogawa), an EMCCD camera (Photometrics Evolve 512; Roper Scientific), and a FRAP/Photoablation scanning system (iLas; Roper Scientific France/The Bio-Imaging Cell and Tissue Core Facility of the Institut Curie). The system was controlled with MetaMorph 7.7 software (Molecular Devices). The microscope was equipped with a custom-ordered illuminator (MEY10021; Nikon) for the attachment of the iLas system. 491 nm (100 mW) Calypso (Cobolt) and 561 nm (100 mW) Jive (Cobolt) lasers were used for excitation. A 355-nm passively Q-switched pulsed laser (Repetition rate 6 kHz, energy/pulse 2.5 mkJ; average power, 13 mW; pick power, 6 kW; pulse width, 400 ps; Teem Photonics) was used for the photo ablation. To keep cells at 37°C, we used a stage top incubator (INUBG2E-ZILCS; Tokai Hit). The 16-bit images were projected onto the CCD chip with intermediate lens 2.0X (Edmund Optics) at a magnification of 0.066 µm/pixel.

Automated image analysis and quantification

To automatically determine the fraction of Vinculin-positive junctions in Figs. 2 c and 4 b, a custom junction detection method was written in MatLab (MathWorks). In this analysis, the VE-cadherin images are background subtracted (Fig. S5 b, left) and segmented in two steps. First, a user defined value is subtracted from the image and the resulting image is used as the marker for grayscale reconstruction to flatten high-intensity areas. In the resulting image, the edges are detected using Sobel's edge detection and areas were filled to obtain a binarized image (Fig. S5 b, step 1). In the second step, a similar grayscale reconstruction image is subtracted from the original. The peaks that are left are segmented using kMeans, binarizing the upper three out of five segments (Fig. S5 b, step 2). The two binary images from these steps are multiplied to determine overlapping areas (Fig. S5 b, right); this method typically detects VE-cadherin–positive fragments of various sizes along the cell–cell contacts. The intensity of Vinculin in each fragment is determined and compared with background, which is the average intensity of a 10-pixel area around that fragment, excluding pixels that belong to neighboring junction fragments. A junction is considered Vinculin positive when the average intensity is 1.5 times above its background.

Immunoprecipitations

Before lysis, cells were stimulated with thrombin for 10 min to maximize the interaction of Vinculin and α-catenin and then lysed at 4°C for 10 min in lysis buffer (1% Nonidet P-40, 25 mM Tris, pH 7.4, 100 mM NaCl, 10 mM $MgCl_2$, 10% glycerol, protease, and phosphatase inhibitors). Lysates were clarified by centrifugation at 14,000 rpm for 1 min. GFP-tagged proteins were precipitated from the lysates using GFP-Trap beads (ChromoTek) for 1 h at 4°C. Precipitations were washed three times in lysis buffer and dissolved in Laemmli sample buffer for standard Western blot analysis.

Statistical analysis

Averages and standard errors of the mean were calculated and are shown in the graphs with corresponding *n* values. P-values are the result of two-tailed, homoscedastic Student's *t* tests.

Online supplemental material

Fig. S1 shows that, in contrast to Vinculin, other focal adhesion markers do not colocalize with cell–cell junctions that are attached to radial actin bundles in IF stainings in HUVECs and HMEC-1s. Fig. S2 shows that Vinculin is recruited to thrombin-induced FAJs in HMEC-1s expressing Vinculin-GFP and p120-catenin–mCherry. Fig. S3 shows single-channel IF images of Fig. 4. Fig. S4 shows that FAJs are disrupted by the addition of Cytochalasin D in HMEC-1s expressing Vinculin-GFP and p120-catenin–mCherry. Fig. S5 a shows that α-catenin–ΔVBS–GFP restores cell–cell adhesion of DLD1-R2/7 α-catenin–negative cells and does not recruit Vinculin to these junctions. Fig. S5 b shows the intermediate steps of image segmentation used in the junction detection method in MatLab. Video 1 shows that remodeling cell–cell junctions adopt a perpendicular orientation in HUVECs expressing VE-cadherin–GFP. Video 2 shows that stable junctions are aligned by, but not directly coupled to, parallel actin bundles, whereas perpendicularly oriented remodeling junctions are attached to radial actin bundles in HUVECs expressing VE-cadherin–GFP and Lifeact-mCherry. Video 3 shows that thrombin strongly induces FAJ formation in HUVECs expressing VE-cadherin–GFP, and Video 4 shows a similar effect of thrombin in HUVECs expressing Vinculin-GFP and p120-catenin–mCherry. Video 5 shows that thrombin transforms stable AJs into FAJs in HUVECs expressing α-catenin–Dendra2 photoswitched at stable AJs. Video 6 shows that Y-27632 inhibits thrombin-induced junction remodeling in HUVECs expressing Vinculin-GFP and p120-catenin–mCherry. Video 7 shows that Cytochalasin D disrupts FAJs but not stable AJs in HUVECs expressing Vinculin-GFP and p120-catenin–mCherry. Video 8 shows tension on FAJs by means of a laser ablation experiment severing radial actin bundles connected to FAJs in HUVECs expressing VE-cadherin–GFP and Lifeact-mCherry. Video 9 shows the junction dynamics of α-catenin–GFP– and α-catenin–ΔVBS–GFP–rescued HUVECs in a knockdown background of endogenous α-catenin. Video 10 shows a comparison of junction remodeling induced by thrombin between normal FAJs and Vinculin-devoid FAJs in α-catenin knockdown HUVECs rescued with α-catenin–GFP or α-catenin–ΔVBS–GFP. Online supplemental material is available at http://www.jcb.org/cgi/content/full/jcb.201108120/DC1.

We thank Jaap van Buul, Akira Nagafuchi, Olivier Pertz, and Frans van Roy for reagents and Hans Bos, Sander Mertens, and Willem-Jan Pannekoek for critically reading the manuscript. We thank Anko de Graaff from the Hubrecht Imaging Center for imaging support. Authors declare no conflicts of interest.

S. Huveneers is supported by the Netherlands Organisation for Scientific Research (NWO)-Veni (project 863.10.003), E. Spanjaard is supported by a grant from the Netherlands Genomics Initiative to J. de Rooij., H. Rehmann is supported by NWO Chemische Wetenschappen (NWO-CW), and J. de Rooij. is supported by grants from the Dutch cancer society (KWF) and NWO-Vidi.

Submitted: 19 August 2011
Accepted: 31 January 2012

References

Abe, K., and M. Takeichi. 2008. EPLIN mediates linkage of the cadherin catenin complex to F-actin and stabilizes the circumferential actin belt. *Proc. Natl. Acad. Sci. USA*. 105:13–19. http://dx.doi.org/10.1073/pnas.0710504105

Abraham, S., M. Yeo, M. Montero-Balaguer, H. Paterson, E. Dejana, C.J. Marshall, and G. Mavria. 2009. VE-Cadherin-mediated cell-cell interaction suppresses sprouting via signaling to MLC2 phosphorylation. *Curr. Biol.* 19:668–674. http://dx.doi.org/10.1016/j.cub.2009.02.057

Allingham, M.J., J.D. van Buul, and K. Burridge. 2007. ICAM-1-mediated, Src- and Pyk2-dependent vascular endothelial cadherin tyrosine phosphorylation is required for leukocyte transendothelial migration. *J. Immunol.* 179:4053–4064.

Angelini, D.J., S.W. Hyun, D.N. Grigoryev, P. Garg, P. Gong, I.S. Singh, A. Passaniti, J.D. Hasday, and S.E. Goldblum. 2006. TNF-alpha increases tyrosine phosphorylation of vascular endothelial cadherin and opens the paracellular pathway through fyn activation in human lung endothelia. *Am. J. Physiol. Lung Cell. Mol. Physiol.* 291:L1232–L1245. http://dx.doi.org/10.1152/ajplung.00109.2006

Bakolitsa, C., D.M. Cohen, L.A. Bankston, A.A. Bobkov, G.W. Cadwell, L. Jennings, D.R. Critchley, S.W. Craig, and R.C. Liddington. 2004. Structural basis for vinculin activation at sites of cell adhesion. *Nature*. 430:583–586. http://dx.doi.org/10.1038/nature02610

Baluk, P., H. Hashizume, and D.M. McDonald. 2005. Cellular abnormalities of blood vessels as targets in cancer. *Curr. Opin. Genet. Dev.* 15:102–111. http://dx.doi.org/10.1016/j.gde.2004.12.005

Bryan, B.A., E. Dennstedt, D.C. Mitchell, T.E. Walshe, K. Noma, R. Loureiro, M. Saint-Geniez, J.P. Campaigniac, J.K. Liao, and P.A. D'Amore. 2010. RhoA/ROCK signaling is essential for multiple aspects of VEGF-mediated angiogenesis. *FASEB J.* 24:3186–3195. http://dx.doi.org/10.1096/fj.09-145102

Carmeliet, P., and R.K. Jain. 2011. Molecular mechanisms and clinical applications of angiogenesis. *Nature*. 473:298–307. http://dx.doi.org/10.1038/nature10144

Chattopadhyay, N., Z. Wang, L.K. Ashman, S.M. Brady-Kalnay, and J.A. Kreidberg. 2003. α3β1 integrin-CD151, a component of the cadherin-catenin complex, regulates PTPmu expression and cell-cell adhesion. *J. Cell Biol.* 163:1351–1362. http://dx.doi.org/10.1083/jcb.200306067

Dejana, E., F. Orsenigo, and M.G. Lampugnani. 2008. The role of adherens junctions and VE-cadherin in the control of vascular permeability. *J. Cell Sci.* 121:2115–2122. http://dx.doi.org/10.1242/jcs.017897

DeMali, K.A., C.A. Barlow, and K. Burridge. 2002. Recruitment of the Arp2/3 complex to vinculin: coupling membrane protrusion to matrix adhesion. *J. Cell Biol.* 159:881–891. http://dx.doi.org/10.1083/jcb.200206043

de Rooij, J., A. Kerstens, G. Danuser, M.A. Schwartz, and C.M. Waterman-Storer. 2005. Integrin-dependent actomyosin contraction regulates epithelial cell scattering. *J. Cell Biol.* 171:153–164. http://dx.doi.org/10.1083/jcb.200506152

Drees, F., S. Pokutta, S. Yamada, W.J. Nelson, and W.I. Weis. 2005. Alpha-catenin is a molecular switch that binds E-cadherin-beta-catenin and regulates actin-filament assembly. *Cell*. 123:903–915. http://dx.doi.org/10.1016/j.cell.2005.09.021

Dudek, S.M., and J.G. Garcia. 2001. Cytoskeletal regulation of pulmonary vascular permeability. *J. Appl. Physiol.* 91:1487–1500.

Esser, S., M.G. Lampugnani, M. Corada, E. Dejana, and W. Risau. 1998. Vascular endothelial growth factor induces VE-cadherin tyrosine phosphorylation in endothelial cells. *J. Cell Sci.* 111:1853–1865.

Fernandez-Borja, M., J.D. van Buul, and P.L. Hordijk. 2010. The regulation of leucocyte transendothelial migration by endothelial signalling events. *Cardiovasc. Res.* 86:202–210. http://dx.doi.org/10.1093/cvr/cvq003

Fischer, R.S., M. Gardel, X. Ma, R.S. Adelstein, and C.M. Waterman. 2009. Local cortical tension by myosin II guides 3D endothelial cell branching. *Curr. Biol.* 19:260–265. http://dx.doi.org/10.1016/j.cub.2008.12.045

Gavard, J., and J.S. Gutkind. 2006. VEGF controls endothelial-cell permeability by promoting the beta-arrestin-dependent endocytosis of VE-cadherin. *Nat. Cell Biol.* 8:1223–1234. http://dx.doi.org/10.1038/ncb1486

He, L., X. Wang, H.L. Tang, and D.J. Montell. 2010. Tissue elongation requires oscillating contractions of a basal actomyosin network. *Nat. Cell Biol.* 12:1133–1142. http://dx.doi.org/10.1038/ncb2124

Humphries, J.D., P. Wang, C. Streuli, B. Geiger, M.J. Humphries, and C. Ballestrem. 2007. Vinculin controls focal adhesion formation by direct interactions with talin and actin. *J. Cell Biol.* 179:1043–1057. http://dx.doi.org/10.1083/jcb.200703036

Imamura, Y., M. Itoh, Y. Maeno, S. Tsukita, and A. Nagafuchi. 1999. Functional domains of alpha-catenin required for the strong state of cadherin-based cell adhesion. *J. Cell Biol.* 144:1311–1322. http://dx.doi.org/10.1083/jcb.144.6.1311

Krishnan, R., D.D. Klumpers, C.Y. Park, K. Rajendran, X. Trepat, J. van Bezu, V.W. van Hinsbergh, C.V. Carman, J.D. Brain, J.J. Fredberg, et al. 2011. Substrate stiffening promotes endothelial monolayer disruption through enhanced physical forces. *Am. J. Physiol. Cell Physiol.* 300:C146–C154. http://dx.doi.org/10.1152/ajpcell.00195.2010

Ladoux, B., E. Anon, M. Lambert, A. Rabodzey, P. Hersen, A. Buguin, P. Silberzan, and R.M. Mège. 2010. Strength dependence of cadherin-mediated adhesions. *Biophys. J.* 98:534–542. http://dx.doi.org/10.1016/j.bpj.2009.10.044

Le Clainche, C., S.P. Dwivedi, D. Didry, and M.F. Carlier. 2010. Vinculin is a dually regulated actin filament barbed end-capping and side-binding protein. *J. Biol. Chem.* 285:23420–23432. http://dx.doi.org/10.1074/jbc.M110.102830

le Duc, Q., Q. Shi, I. Blonk, A. Sonnenberg, N. Wang, D. Leckband, and J. de Rooij. 2010. Vinculin potentiates E-cadherin mechanosensing and is recruited to actin-anchored sites within adherens junctions in a myosin II-dependent manner. *J. Cell Biol.* 189:1107–1115. http://dx.doi.org/10.1083/jcb.201001149

Liu, Z., J.L. Tan, D.M. Cohen, M.T. Yang, N.J. Sniadecki, S.A. Ruiz, C.M. Nelson, and C.S. Chen. 2010. Mechanical tugging force regulates the size of cell-cell junctions. *Proc. Natl. Acad. Sci. USA*. 107:9944–9949. http://dx.doi.org/10.1073/pnas.0914547107

Maddugoda, M.P., M.S. Crampton, A.M. Shewan, and A.S. Yap. 2007. Myosin VI and vinculin cooperate during the morphogenesis of cadherin cell–cell contacts in mammalian epithelial cells. *J. Cell Biol.* 178:529–540. http://dx.doi.org/10.1083/jcb.200612042

Mammoto, A., T. Mammoto, and D.E. Ingber. 2008. Rho signaling and mechanical control of vascular development. *Curr. Opin. Hematol.* 15:228–234. http://dx.doi.org/10.1097/MOH.0b013e3282fa7445

McKenzie, J.A., and A.J. Ridley. 2007. Roles of Rho/ROCK and MLCK in TNF-alpha-induced changes in endothelial morphology and permeability. *J. Cell. Physiol.* 213:221–228. http://dx.doi.org/10.1002/jcp.21114

Mierke, C.T., P. Kollmannsberger, D.P. Zitterbart, J. Smith, B. Fabry, and W.H. Goldmann. 2008. Mechano-coupling and regulation of contractility by the vinculin tail domain. *Biophys. J.* 94:661–670. http://dx.doi.org/10.1529/biophysj.107.108472

Millán, J., R.J. Cain, N. Reglero-Real, C. Bigarella, B. Marcos-Ramiro, L. Fernández-Martín, I. Correas, and A.J. Ridley. 2010. Adherens junctions connect stress fibres between adjacent endothelial cells. *BMC Biol.* 8:11. http://dx.doi.org/10.1186/1741-7007-8-11

Miyake, Y., N. Inoue, K. Nishimura, N. Kinoshita, H. Hosoya, and S. Yonemura. 2006. Actomyosin tension is required for correct recruitment of adherens junction components and zonula occludens formation. *Exp. Cell Res.* 312:1637–1650. http://dx.doi.org/10.1016/j.yexcr.2006.01.031

Moy, A.B., J. Van Engelenhoven, J. Bodmer, J. Kamath, C. Keese, I. Giaever, S. Shasby, and D.M. Shasby. 1996. Histamine and thrombin modulate endothelial focal adhesion through centripetal and centrifugal forces. *J. Clin. Invest.* 97:1020–1027. http://dx.doi.org/10.1172/JCI118493

Peng, X., L.E. Cuff, C.D. Lawton, and K.A. DeMali. 2010. Vinculin regulates cell-surface E-cadherin expression by binding to beta-catenin. *J. Cell Sci.* 123:567–577. http://dx.doi.org/10.1242/jcs.056432

Puklin-Faucher, E., and M.P. Sheetz. 2009. The mechanical integrin cycle. *J. Cell Sci.* 122:179–186. http://dx.doi.org/10.1242/jcs.042127

Rauzi, M., P.F. Lenne, and T. Lecuit. 2010. Planar polarized actomyosin contractile flows control epithelial junction remodelling. *Nature*. 468:1110–1114. http://dx.doi.org/10.1038/nature09566

Riedl, J., A.H. Crevenna, K. Kessenbrock, J.H. Yu, D. Neukirchen, M. Bista, F. Bradke, D. Jenne, T.A. Holak, Z. Werb, et al. 2008. Lifeact: a versatile marker to visualize F-actin. *Nat. Methods*. 5:605–607. http://dx.doi.org/10.1038/nmeth.1220

Rodríguez Fernández, J.L., B. Geiger, D. Salomon, and A. Ben-Ze'ev. 1993. Suppression of vinculin expression by antisense transfection confers changes in cell morphology, motility, and anchorage-dependent growth of 3T3 cells. *J. Cell Biol.* 122:1285–1294. http://dx.doi.org/10.1083/jcb.122.6.1285

Shasby, D.M., T. Stevens, D. Ries, A.B. Moy, J.M. Kamath, A.M. Kamath, and S.S. Shasby. 1997. Thrombin inhibits myosin light chain dephosphorylation in endothelial cells. *Am. J. Physiol.* 272:L311–L319.

Taguchi, K., T. Ishiuchi, and M. Takeichi. 2011. Mechanosensitive EPLIN-dependent remodeling of adherens junctions regulates epithelial reshaping. *J. Cell Biol.* 194:643–656. http://dx.doi.org/10.1083/jcb.201104124

Tzima, E., M. Irani-Tehrani, W.B. Kiosses, E. Dejana, D.A. Schultz, B. Engelhardt, G. Cao, H. DeLisser, and M.A. Schwartz. 2005. A mechanosensory complex that mediates the endothelial cell response to fluid shear stress. *Nature*. 437:426–431. http://dx.doi.org/10.1038/nature03952

van Hengel, J., L. Gohon, E. Bruyneel, S. Vermeulen, M. Cornelissen, M. Mareel, and F. von Roy. 1997. Protein kinase C activation upregulates intercellular adhesion of α-catenin–negative human colon cancer cell variants via induction of desmosomes. *J. Cell Biol.* 137:1103–1116. http://dx.doi.org/10.1083/jcb.137.5.1103

van Nieuw Amerongen, G.P., S. van Delft, M.A. Vermeer, J.G. Collard, and V.W. van Hinsbergh. 2000. Activation of RhoA by thrombin in endothelial hyperpermeability: role of Rho kinase and protein tyrosine kinases. *Circ. Res.* 87:335–340.

Vasioukhin, V., C. Bauer, M. Yin, and E. Fuchs. 2000. Directed actin polymerization is the driving force for epithelial cell-cell adhesion. *Cell*. 100:209–219. http://dx.doi.org/10.1016/S0092-8674(00)81559-7

Vestweber, D., M. Winderlich, G. Cagna, and A.F. Nottebaum. 2009. Cell adhesion dynamics at endothelial junctions: VE-cadherin as a major player. *Trends Cell Biol.* 19:8–15. http://dx.doi.org/10.1016/j.tcb.2008.10.001

Watabe-Uchida, M., N. Uchida, Y. Imamura, A. Nagafuchi, K. Fujimoto, T. Uemura, S. Vermeulen, F. van Roy, E.D. Adamson, and M. Takeichi. 1998. α-Catenin–vinculin interaction functions to organize the apical junctional complex in epithelial cells. *J. Cell Biol.* 142:847–857. http://dx.doi.org/10.1083/jcb.142.3.847

Weis, S.M. 2008. Vascular permeability in cardiovascular disease and cancer. *Curr. Opin. Hematol.* 15:243–249. http://dx.doi.org/10.1097/MOH.0b013e3282f97d86

Weis, W.I., and W.J. Nelson. 2006. Re-solving the cadherin-catenin-actin conundrum. *J. Biol. Chem.* 281:35593–35597. http://dx.doi.org/10.1074/jbc.R600027200

Wen, K.K., P.A. Rubenstein, and K.A. DeMali. 2009. Vinculin nucleates actin polymerization and modifies actin filament structure. *J. Biol. Chem.* 284:30463–30473. http://dx.doi.org/10.1074/jbc.M109.021295

Yamada, S., and W.J. Nelson. 2007. Localized zones of Rho and Rac activities drive initiation and expansion of epithelial cell–cell adhesion. *J. Cell Biol.* 178:517–527. http://dx.doi.org/10.1083/jcb.200701058

Yamada, S., S. Pokutta, F. Drees, W.I. Weis, and W.J. Nelson. 2005. Deconstructing the cadherin-catenin-actin complex. *Cell*. 123:889–901. http://dx.doi.org/10.1016/j.cell.2005.09.020

Yonemura, S., M. Itoh, A. Nagafuchi, and S. Tsukita. 1995. Cell-to-cell adherens junction formation and actin filament organization: similarities and differences between non-polarized fibroblasts and polarized epithelial cells. *J. Cell Sci.* 108:127–142.

Yonemura, S., Y. Wada, T. Watanabe, A. Nagafuchi, and M. Shibata. 2010. alpha-Catenin as a tension transducer that induces adherens junction development. *Nat. Cell Biol.* 12:533–542. http://dx.doi.org/10.1038/ncb2055

Zeng, H., D. Zhao, and D. Mukhopadhyay. 2002. KDR stimulates endothelial cell migration through heterotrimeric G protein Gq/11-mediated activation of a small GTPase RhoA. *J. Biol. Chem.* 277:46791–46798. http://dx.doi.org/10.1074/jbc.M206133200